

Oxide formation at the surface of late 4d transition metals: Insights from *first-principles atomistic thermodynamics*

Karsten Reuter^{1,2} and Matthias Scheffler¹

¹ *Fritz-Haber-Institut der Max-Planck-Gesellschaft,
Faradayweg 4-6, D-14195 Berlin-Dahlem, Germany and*

² *FOM Institute for Atomic and Molecular Physics,
Kruislaan 407, 1098 SJ Amsterdam (The Netherlands)*

(Dated: Received: 24 March 2003)

Using density-functional theory we assess the stability of bulk and surface oxides of the late 4d transition metals in a “constrained equilibrium” with a gas phase formed of O₂ and CO. While the stability range of the most stable bulk oxide extends for ruthenium well into gas phase conditions representative of technological CO oxidation catalysis, this is progressively less so for the 4d metals to its right in the periodic system. Surface oxides could nevertheless still be stable under such conditions. These thermodynamic considerations are discussed in the light of recent experiments, emphasizing the role of (surface) oxides as the active phase of model catalysts formed from these metals.

PACS numbers: PACS: 82.65.Mq, 68.35.Md, 68.43.Bc

I. INTRODUCTION

Rhodium and palladium exhibit a high reactivity for the CO oxidation reaction, which has led to their widespread use in catalytic car exhaust converters¹. The degree of oxidation of these materials in the reactive environment has been a frequent object of speculation in the experimental catalysis literature (see e.g. refs. 2,3,4,5,6,7,8), with oxide formation at the surface of the metal particles potentially having either beneficial or detrimental effects on the overall activity. Lacking microscopic *in-situ* data to really resolve this issue a possibly beneficial role has e.g. been suspected for PdO at Pd⁷, whereas Rhodium oxides have predominantly been viewed as poisoning the catalytic reaction^{2,3,4}.

While the atomic-scale techniques of Ultra High Vacuum (UHV) surface-science would in principle be able to provide additional insight into this subject matter, formation of oxides in particular of the more noble metals was often neglected in corresponding works, partly due to the fact that these oxides form only at rather high oxygen pressures and elevated temperatures. This emphasis on metallic substrates has changed over the last years, bringing oxide surfaces now also on the agenda of surface-science studies attempting to bridge the pressure gap between UHV and technological oxidation catalysis⁹. Concomitantly, on Ru(0001)^{10,11}, Pd(100)^{12,13}, and Ag(111)^{14,15} oxygen-rich environmental conditions were reported to lead to oxide (or “surface oxide”) formation, in all cases connected with a significant increase in catalytic activity.

This new focus on the effect of the environment on surface structure and reactivity is intertwined with corresponding theoretical efforts. In particular the concept of *first-principles atomistic thermodynamics*^{16,17,18,19} has recently proven to be most valuable for the study of oxide surfaces (see e.g. refs. 20,21,22,23,24). In this branch of

thermodynamics density-functional theory (DFT) is employed to compute free energies, in order to identify the lowest-energy atomic structure for a given condition of thermodynamic reservoirs representing the surrounding gas phase, and possibly combining this with constraints to facilitate the analysis^{23,24}. In the following we will use and describe this formalism to discuss the stability of bulk and surface oxides of the late 4d transition metals (TMs) Ru, Rh, Pd, and Ag. The results of these very basic thermodynamic considerations are found to nicely embrace the aforescribed existing experimental data, e.g. pointing at the relevance of thin surface oxide layers on Pd under the conditions of high-pressure CO oxidation catalysis.

II. “CONSTRAINED THERMODYNAMICS”

The question we like to ask in this context is, given a certain gas phase environment composed of O₂ and CO, does a bulk or surface oxide of the late 4d TMs form a stable phase? In a thermodynamic description we then resort to some form of equilibrium that exists between various components i in the system, all of which are present in sufficient quantities. Under conditions of constant temperature, T , and pressures, $\{p_i\}$, this allows to discuss relations between the respective reservoirs, characterized by their chemical potentials $\mu_i(T, p_i)$ or Gibbs free energies $g_i(T, p_i)$. For a gas phase composed of CO and O₂ a forthright assumption of full equilibrium does, however, not yield a description suitable for our interest in oxidation catalysis: From energy considerations alone, CO₂ would then result as the most stable gas phase molecule for almost all temperature and pressure conditions. On the other hand, because of the large free energy barrier for the gas phase reaction $\text{CO} + 1/2 \text{O}_2 \rightarrow \text{CO}_2$, such a full equilibrium will not be attained on

time scales relevant to us. Instead, we may ignore CO₂ formation in the gas phase and consider the presence of two separate, independent reservoirs for O₂ and CO in the environment. While both components are therefore not in equilibrium with each other, each one is individually assumed in equilibrium with either the metal (M) or the oxide (M_xO_y) phase.

As a consequence the chemical potentials of both oxygen and CO in the whole system are then determined by the surrounding gas phase reservoirs, i.e. their temperature and pressure dependence is given by^{22,24}

$$\mu_{\text{O}}(T, p_{\text{O}_2}) = \frac{1}{2} \left[E_{\text{O}_2}^{\text{total}} + \tilde{\mu}_{\text{O}_2}(T, p^0) + k_{\text{B}} T \ln \left(\frac{p_{\text{O}_2}}{p^0} \right) \right], \quad (1)$$

and

$$\mu_{\text{CO}}(T, p_{\text{CO}}) = E_{\text{CO}}^{\text{total}} + \tilde{\mu}_{\text{CO}}(T, p^0) + k_{\text{B}} T \ln \left(\frac{p_{\text{CO}}}{p^0} \right), \quad (2)$$

where the temperature dependence of $\tilde{\mu}_{\text{O}_2}(T, p^0)$ and $\tilde{\mu}_{\text{CO}}(T, p^0)$ includes the contributions from vibrations and rotations of the molecules, as well as the ideal gas entropy at $p^0 = 1$ atmosphere. The latter quantities can be computed from first principles, yielding results that are at the temperature range of interest to us virtually indistinguishable from the experimental values listed in thermodynamic tables^{24,25}. Via eqs. (1) and (2) our results obtained as a function of the chemical potentials, i.e. in $(\mu_{\text{O}}, \mu_{\text{CO}})$ -space, can then be converted into pressure scales at any specific temperature. Roughly representing the temperature range relevant to our study, this will be illustrated with specific scales at $T = 300$ K and $T = 600$ K in all figures below.

In the resulting “constrained equilibrium” situation^{23,24} the only pathway to CO₂ formation is due to a reduction of the oxide or due to the catalytic CO oxidation at the substrate surface. In a flow reactor this constant build-up of CO₂ is counteracted by the continuous stream (and thus removal) of gases over the catalyst surface, yielding a CO₂ concentration gradient under stationary operation conditions. Although formed CO₂ molecules may in principle readsorb at the surface (dissociatively or as a molecule), the probability of this event is very low compared to the much more frequent O₂ and CO (re)adsorption. The surface is therefore unlikely to equilibrate with the surrounding CO₂ gas phase, and a proper description would have to involve a dynamical treatment of the CO₂ gas flow close to the catalyst surface. Such treatment will be published elsewhere²⁶. Here we use a very simple estimate for the CO₂ free energy, namely the internal energy of a free CO₂ molecule. The error introduced by this estimate will vary from material to material, but in our preliminary kinetic Monte Carlo simulations for RuO₂(110) we find it to be small.²⁶

Although crude, this approximation is appropriate for the present trend study aiming only at a first assessment of oxide stability, and an uncertainty of some tenths of eV

does not change the nature of our conclusions. In this respect we stress that the whole concept of a “constrained equilibrium” is not designed to yield precise answers to the microscopic state and reactivity of the catalyst surface. For that, the very dynamic behavior must be modeled by statistical mechanics. Yet, with atomistic thermodynamics one can trace out the large scale behavior and identify those conditions where such a more refined treatment is necessary.

III. BULK OXIDE STABILITY

If there is a pure oxygen environment, the condition for the stability of the bulk oxide is

$$g_{\text{M}_x\text{O}_y}^{\text{bulk}} < x g_{\text{M}}^{\text{bulk}} + y \mu_{\text{O}}, \quad (3)$$

i.e.

$$\Delta\mu_{\text{O}} > \frac{1}{y} \left[g_{\text{M}_x\text{O}_y}^{\text{bulk}} - x g_{\text{M}}^{\text{bulk}} - \frac{y}{2} E_{\text{O}_2}^{\text{total}} \right]. \quad (4)$$

Here $\Delta\mu_{\text{O}}$ is defined as $\mu_{\text{O}} - (1/2)E_{\text{O}_2}^{\text{total}}$. For $T = 0$ K the bracket on the right hand side equals half of the low temperature limit of the heat of formation, $H_f(T = 0 \text{ K}, p = 0)$. Even for higher temperatures this will not change substantially as for bulk phases the (T, p) -dependence of their Gibbs free energies is rather small, i.e. the right hand side will still be rather close to the $H_f(T = 0 \text{ K}, p = 0)$ -value and not follow the pronounced variation of $H_f(T, p)$ (which is primarily due to the (T, p) -dependence of the μ_{O_2} -term, while only $E_{\text{O}_2}^{\text{total}}$ enters the right hand side of eq. (4)). We therefore replace the bracket in eq. (4) by $(1/y)H_f(T = 0 \text{ K})$ and arrive at our first stability condition

$$\Delta\mu_{\text{O}} \gtrsim \frac{1}{y} H_f(T = 0 \text{ K}). \quad (5)$$

Additionally, the oxide can also be destroyed (reduced) by carbon monoxide. In a pure CO environment, the stability condition for the oxide is

$$g_{\text{M}_x\text{O}_y}^{\text{bulk}} + y \mu_{\text{CO}} < x g_{\text{M}}^{\text{bulk}} + y \mu_{\text{CO}_2}. \quad (6)$$

Following the discussion above we will crudely approximate μ_{CO_2} in the present study by the internal energy of a free CO₂ molecule. In a similar fashion as for the pure oxygen environment one can then simplify the stability condition to

$$\Delta\mu_{\text{CO}} \lesssim -\frac{1}{y} H_f(T = 0 \text{ K}) + \Delta E^{\text{mol.}}, \quad (7)$$

introducing $\Delta\mu_{\text{CO}} = \mu_{\text{CO}} - E_{\text{CO}}^{\text{total}}$ and using the short hand $\Delta E^{\text{mol.}} = (E_{\text{CO}_2}^{\text{bind}} - E_{\text{CO}}^{\text{bind}} - 1/2 E_{\text{O}_2}^{\text{bind}})$ for the difference in binding energies of the three gas phase molecules. As described in detail in a previous publication²⁴ our DFT computations including zero-point vibrations give

TABLE I: Low-temperature limit of the heat of formation, $\Delta H_f(T = 0\text{ K})$, of the most stable bulk oxide of the four late 4d transition metals from DFT and from experiment. The DFT values do not include the zero-point energies of the solid phases.

	Theory	Experiment
RuO ₂	-3.4 eV ²²	-3.19 eV ²⁷
Rh ₂ O ₃	-3.8 eV ²⁸	-3.57 eV ²⁷
PdO	-0.9 eV ²⁹	-0.88 eV ²⁷
Ag ₂ O	-0.2 eV ¹⁵	-0.34 eV ²⁷

$\Delta E^{\text{mol.}} = -3.2\text{ eV}$, which agrees well with the experimental value of -2.93 eV ²⁵. Although state-of-the-art DFT total energies of the O₂ molecule are subject to a noticeable error, some cancellation apparently occurs for the composite quantity $\Delta E^{\text{mol.}}$, rendering it rather unimportant on the scale of the present study whether the experimental or theoretical value for $\Delta E^{\text{mol.}}$ is used.

Finally, if O₂ and CO are both present in the gas phase in “constrained equilibrium” with the oxide, then the general stability condition is simply obtained by combining eqs. (5) and (7) for the separate cases:

$$\Delta\mu_{\text{CO}} - \Delta\mu_{\text{O}} \lesssim -\frac{2}{y}H_f(T = 0\text{ K}) + \Delta E^{\text{mol.}}, \quad (8)$$

while eq. (5) still applies for very low CO concentrations. Hence, in both conditions for the stability of the bulk oxide, eqs. (5) and (8), the only quantity left to determine is $\Delta H_f(T = 0\text{ K})$. This value has been computed in previous works^{15,22,28,29} and we content ourselves here with simply listing the DFT values for the most stable oxides of the four late 4d TMs in Table I, again comparing with the low-temperature limit of the experimental heat of formation²⁷. Keeping the sizable error in the O₂ DFT total energy in mind, we notice in all cases a fortuitous error cancellation, leading again to rather small differences when evaluating the stability conditions with either experimental or theoretical numbers. Only in the case of silver oxide has $\Delta H_f(T = 0\text{ K})$ become so small that this error becomes somewhat disturbing (in particular for the stability condition in eq. (8)). More refined treatments for approximating the stability conditions, e.g. including entropic contributions to $\Delta H_f(T, p)$, can be devised¹⁵, but for our present purposes it suffices to see that bulk Ag₂O has such a low stability that it will not play a role in our further discussion.

The derived (T, p) -ranges for stability of the 4d bulk oxides are shown in Fig. 1, exhibiting a pronounced decrease from RuO₂ towards the oxides of the metals to its right in the periodic system. We stress that the aforesaid crude treatment of the CO₂ free energy translates into rather large error bars on the diagonal lines running from bottom left to top right in the figure (i.e. the limit due to the stability condition of eq. (8)). The uncertainty in μ_{CO_2} translates directly into the height of these lines, which with the present error estimate could therefore be shifted up or down by some tenths of an eV.

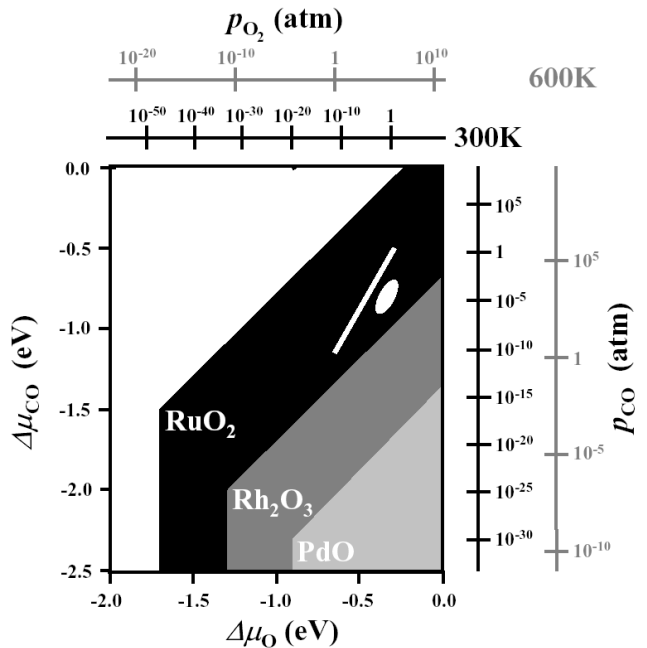


FIG. 1: Stability regions of bulk oxides of the late 4d transition metals in $(\Delta\mu_{\text{O}}, \Delta\mu_{\text{CO}})$ -space, on the basis of the DFT data listed in Table I. Additionally, pressure scales are drawn for $T = 300\text{ K}$ and $T = 600\text{ K}$. The white line indicates conditions corresponding to $p_{\text{O}} = p_{\text{CO}} = 1\text{ bar}$ and $300\text{ K} \leq T \leq 600\text{ K}$, and environments relevant for CO oxidation catalysis over these metals would correspond to the near vicinity of this line. More specifically, the small white area indicates roughly the (T, p) -conditions employed in a recent experimental study by Hendriksen and Frenken (see text)^{13,38}. The stability of Ag₂O is so low, that it does not appear any more within the limits considered here. We stress that the rough treatment of the CO₂ free energy translates into an uncertainty in the position of the diagonal lines (which could be shifted up or down by some tenths of an eV).

IV. SURFACE OXIDE STABILITY

Deferring the discussion of the derived bulk oxide stability to the end of this paper, we proceed to analyze in the stability context a second, only recently emphasized aspect of metal oxidation, namely the formation of thin surface oxides. While traditionally such films were conceived as closely-related thin versions of the corresponding bulk oxides, recent atomic scale characterizations of initial few-atom thick oxide overlayers especially on Pd and Ag surfaces revealed structures that had only little resemblance to their bulk counterparts, and/or were to a large degree influenced by a strong coupling to the underlying metal substrate^{14,30,31}. Due to this coupling and structures particularly suited for layered configurations, one may expect the stability range for such surface oxides to exceed that of the hitherto discussed bulk oxides.

To determine the range of (T, p) -conditions in which a surface oxide would represent the thermodynamically most stable state, we follow the approach of Li, Stampfl

and Scheffler¹⁵, i.e. we evaluate the Gibbs free energy of adsorption and compare it to other possible states of the system like on- or sub-surface oxygen phases or the bulk oxide. For the case of a pure O₂ environment and using the same approximations as discussed in the last section, we may write this Gibbs free energy of adsorption as

$$\begin{aligned} \Delta G(\Delta\mu_{\text{O}}) &\approx \\ &\approx -\frac{1}{A} \left(E_{\text{O@M}}^{\text{total}} - E_{\text{M}}^{\text{total}} - N_{\text{O}} \left(\frac{1}{2} E_{\text{O}_2}^{\text{total}} + \Delta\mu_{\text{O}} \right) \right) \\ &= \frac{N_{\text{O}}}{A} (E_{\text{O@M}}^{\text{bind}} + \Delta\mu_{\text{O}}). \end{aligned} \quad (9)$$

Here, $E_{\text{O@M}}^{\text{total}}$ and $E_{\text{M}}^{\text{total}}$ are the total energies of the surface with and without oxygen coverage of N_{O} oxygen atoms per surface area A . In the second line, we have identified the first terms in the brackets with the average binding energy of oxygen in the particular surface configuration and with respect to $1/2 E_{\text{O}_2}^{\text{total}}$.

Obviously, the higher the oxygen content of a considered surface structure, the steeper its $\Delta G(\Delta\mu_{\text{O}})$ will decrease with increasing chemical potential. In the limiting case of an infinitely thick bulk oxide on top of the metal substrate, this will result in a vertical line that crosses the zero-axis at the stability condition for the bulk oxide in eq. (5). For any higher $\Delta\mu_{\text{O}}$ the bulk oxide will be the stable phase, but the interesting question is to see whether there are lower $\Delta\mu_{\text{O}}$ than this limit, for which the lines of a surface oxide structure turn out lower than e.g. on-surface adsorption or the clean surface corresponding to $\Delta G(\Delta\mu_{\text{O}}) = 0$.

We exemplify this ansatz by first analyzing the stability of a surface oxide on Pd(100). In addition to the well known $p(2 \times 2)$ and $c(2 \times 2)$ ordered adlayers with O in fcc sites^{33,34}, an ensuing $(\sqrt{5} \times \sqrt{5})R27^\circ$ -O surface oxide phase on this surface was recently characterized as a rumpled, but commensurate PdO(101) film with a strong coupling to the underlying Pd(100) substrate^{31,32}. Evaluating the reported binding energies in this study with eq. (9) we obtain the results displayed in Fig. 2. Interestingly, the $\Delta\mu_{\text{O}}$ -range where this surface oxide exhibits the lowest Gibbs free energy of adsorption not only exceeds the one of the aforesaid PdO bulk oxide, but also the range where the on-surface adsorption phases are more stable than the clean Pd(100) surface. In other words, the latter on-surface phases never correspond to a thermodynamically stable phase, and their frequent observation in UHV experiments^{33,34} appears to be a mere outcome of the limited O supply offered, as well as of kinetic barriers e.g. for O penetration at the low temperatures employed (UHV experiments are typically performed by depositing a finite number of adatoms, rather than by maintaining a given gas pressure).

It is interesting to compare these findings with the equivalent situation on another Pd surface orientation. On Pd(111), a surface oxide not resembling the bulk-structure of PdO at all was recently reported as the product of high oxygen exposure and following the well-

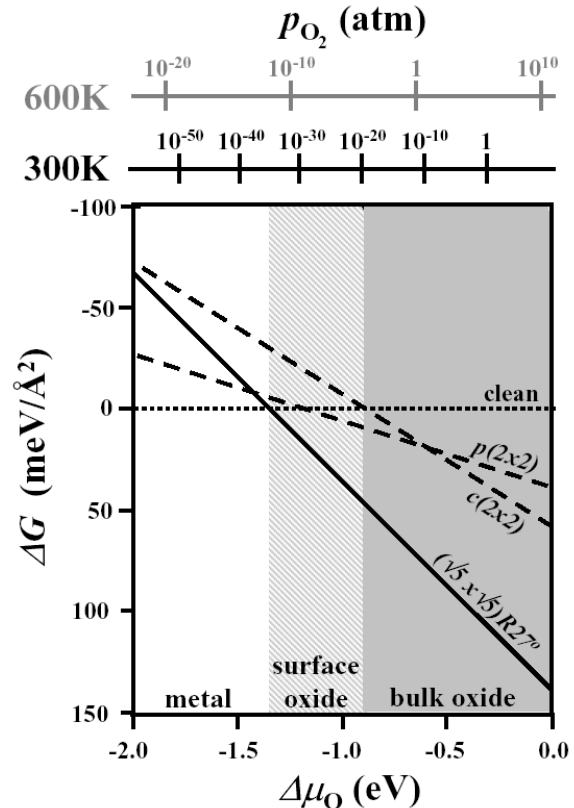


FIG. 2: Computed Gibbs free energy of adsorption for the $p(2 \times 2)$ and $c(2 \times 2)$ on-surface adsorption phase, as well as for the $(\sqrt{5} \times \sqrt{5})R27^\circ$ -O surface oxide on Pd(100). The surface unit cell of Pd(100) is 7.8 \AA^2 . The stability range of the surface oxide extends well beyond that of the bulk oxide, given by $\Delta\mu_{\text{O}} \gtrsim -0.9 \text{ eV}$, cf. eq. (5). The dependence on $\Delta\mu_{\text{O}}$ is again translated into pressure scales at $T = 300 \text{ K}$ and $T = 600 \text{ K}$ for clarity. In the bottom of the figure, the “material type” which is stable in the corresponding range of O chemical potential is listed and indicated by the shaded regions. The binding energies used to construct this graph are taken from refs. 31,32.

studied $p(2 \times 2)$ on-surface adsorption phase³⁰. Using the DFT binding energies provided in this study to evaluate eq. (9), we again obtain a range of (T, p) -conditions outside of the bulk oxide stability range, for which this surface oxide phase is most stable as shown in Fig. 3. This time, however, this range extends only within $-1.2 \text{ eV} \gtrsim \Delta\mu_{\text{O}} \gtrsim -0.9 \text{ eV}$, below which first the on-surface adsorption phase and then the clean Pd(111) surface becomes more stable. If we compare this to the results shown in Fig. 2, there are thus environmental conditions, in which a surface oxide may already be thermodynamically stable on Pd(100), while on-surface adsorption still prevails on Pd(111). Knowing that these two surfaces form the predominant surface area of Pd nanoparticles³⁵, this may have profound consequences on the oxidation behavior of the latter and we will return to this point

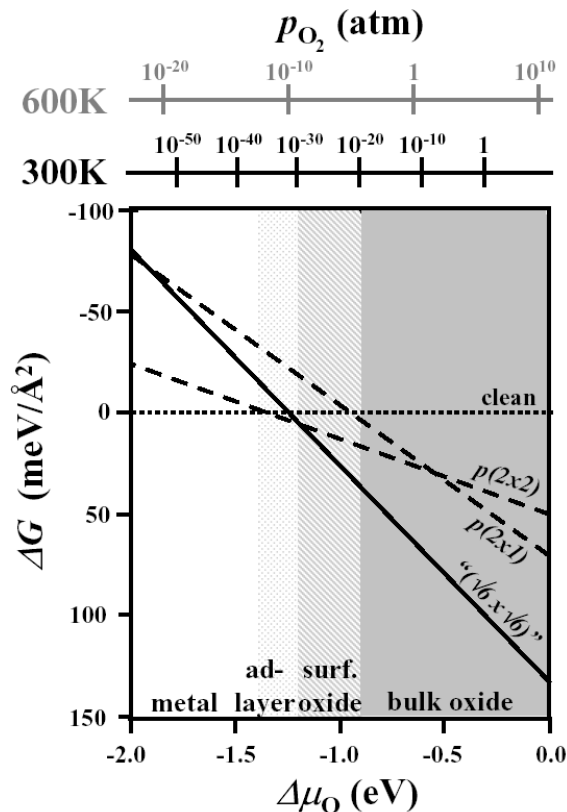


FIG. 3: Computed Gibbs free energy of adsorption for the $p(2 \times 2)$ and hypothetical $p(2 \times 1)$ on-surface adsorption phase, as well as for the so-called $(\sqrt{6} \times \sqrt{6})$ -O surface oxide on Pd(111). The surface unit cell of Pd(111) is 6.7 \AA^2 . Again, the stability range of the surface oxide extends beyond that of the bulk oxide, cf. Fig. 2, but this time there is also a finite range in which an adlayer forms the thermodynamically most stable phase. The binding energies used to construct this graph are taken from ref. 30.

below.

While a similar situation with the commensurable $p(4 \times 4)$ surface oxide¹⁴ slightly exceeding the stability range of bulk Ag_2O was also found for $\text{Ag}(111)$ ¹⁵, no (T, p) -range most favorable for the various intermediate precursors suggested in the oxidation pathway from $\text{Ru}(0001)$ to $\text{RuO}_2(110)$ is obtained when evaluating the DFT binding energies reported in the corresponding refs. 36,37. Tentatively, we therefore expect surface oxides to play a thermodynamic role more for the $4d$ TMs towards the right of the periodic system, where the decreasing thermal stability of the bulk oxides and the lowered bulk modulus of oxide and metal phase enhances the influence of oxide-metal coupling, and thus the tendency to form commensurable, even non-bulk like surface oxide configurations. It is interesting to notice that the extended stability range of the surface oxide phase discussed on Pd(100), cf. Fig. 2, corresponds more or less to the range exhibited by bulk Rh_2O_3 in Fig. 1, i.e. it comes now rather close to the schematically indicated range

of $(T, p_{\text{O}}, p_{\text{CO}})$ -conditions representative of technological CO oxidation catalysis.

V. IMPLICATIONS FOR THE CATALYTIC CO OXIDATION

Due to the particular construction of our “constrained equilibrium” approach we could expect the results summarized in Figs. 1 to 3 to give a rough reflection of the state of the catalyst during steady-state CO oxidation, as long as kinetic effects both in the formation of the (surface) oxides themselves, as well as in the ongoing reaction on the surface (e.g. possibly consuming oxygen more rapidly than it is replenished) are negligible²⁶. Although technological catalysis typically operates well above room temperature, such effects can never be ruled out in general. Clearly, a comprehensive understanding of the full catalytic activity and the microscopic state of the catalyst (i.e. its very dynamic behavior) requires modeling by statistical mechanics, and the results of thermodynamic considerations must consequently be treated with great care. Still, we believe that our results may be employed for a first qualitative assessment of oxide formation on the late $4d$ TMs, in particular if supplemented by some already known kinetic constraints.

In this regard we first notice the rather large stability range of bulk RuO_2 , extending well over the whole range of environmental conditions relevant for technological CO oxidation catalysis, cf. Fig. 1. Rather high temperatures of the order of $T \sim 600 \text{ K}$ are required to form this bulk oxide^{10,11}, which would explain the recently reported lack of oxide formation at $\text{Ru}(0001)$ even under high pressure conditions at temperatures around $T \sim 400 \text{ K}$ ^{13,38}. Yet, once this bulk oxide is formed, our thermodynamic results imply that the catalytic activity of Ru catalysts might in reality be due to oxides, in line with the results of a number of recent experimental studies^{9,10,11}.

For Rh the stability range of its bulk oxide has already decreased significantly. Even if the catalyst was in a situation close to thermodynamic equilibrium, our results suggest that either metal or bulk oxide could prevail at technologically relevant environmental conditions, depending on the exact partial pressures and temperature in the gas phase, i.e. depending on whether one is below or above the stability line in Fig. 1 (and recall that the present uncertainty in the location of this line is some tenths of eV). Even more intriguing, oscillations between the two phases could result as a consequence of fluctuations, when operating under environmental conditions very close to the stability line of Rh_2O_3 . Similar considerations might also be possible for Pd, yet this time not concerning transitions to bulk PdO (which is already far too unstable), but to thin oxide films limited to the very surface region - as mentioned in section IV the stability of the surface oxide on Pd(100) extends over a similar range to that of bulk Rh_2O_3 in Fig. 1. In this respect we have also roughly marked in Fig. 1

the (T, p) -conditions employed in a recent experimental study on Pd(100), where a substantial roughening of the surface with presumed constant formation and reduction of ultra-thin oxide domains during the CO oxidation reaction was reported^{12,13}. The closeness of these experimental environmental conditions with our rough instability estimate for the surface oxide on Pd(100) is startling, in particular when further recalling the frequent observation of spatio-temporal pattern formation during the CO reaction at other Pd surfaces like Pd(110), which was there also connected to reversible oxide formation and reduction⁶.

At this stage it is worth digressing on the fact that such thin oxide films with possibly even fluctuating conditions at the catalyst surface are tough to describe (even conceptually) within the traditional language of generic reaction mechanisms (see e.g. ref. 39 for a review). For metal surfaces mostly a Langmuir-Hinshelwood (LH) type behavior is discussed, where both reactants adsorb at the surface first and react thereafter. For the case of oxidation reactions on oxide surfaces on the other hand, Mars and van Krevelen (MvK)⁴⁰ suggested that the underlying substrate itself might become continually reduced and (re-)oxidized in the on-going reaction, i.e. that oxygen from the oxide lattice is consumed in the reaction and then replenished from the gas phase. Within the framework of macroscopic rate equations, where this approach was made and has ever since been very popular (in the oxide literature), this translates to relaxing the constraint of a fixed number of active surface sites underlying the LH kinetics. The resulting MvK rate equation is then similar, but not identical to the one derived for a LH reaction mechanism, although in actual practice most data can be fitted equally well with both rate equations³⁹.

This only vague distinction between both mechanisms becomes even more blurred when starting to think microscopically and particularly when considering what is now called a surface oxide (a 1-2 layer thick oxide-like film). For the case of a fixed oxide lattice, where certain surface oxygen atoms just take part in the reaction and the resulting vacancies are refilled afterwards, a distinction between LH and MvK is in fact just semantics: One could equally well view the oxide lattice with the created vacancies (thus MvK) as the real substrate, where then oxygen adsorbs into these sites and reacts thereafter (thus LH). Although such a scenario has been advocated as a MvK mechanism for CO oxidation on RuO₂(110)¹⁰, one might even argue that it contradicts the original MvK definition in its strictest sense, which emphasized the non-finite number of active sites (that is certainly fixed by the number of surface oxygen sites in the latter situation).

Other interpretations of MvK have therefore focused more on a diffusional aspect that would arise if oxygen is consumed at one point of the lattice surface but replenished elsewhere, requiring some form of oxygen transport in or at the surface (that might even become rate-limiting and thus yield a new type of kinetics)⁴¹. Nevertheless, a

clearcut distinction could even then not always be made. Picturing in particular a possibly only one-layer thick oxide film, that does not necessarily resemble a bulk-like oxide structure at all, or the aforescribed situation of a surface close to an instability with a continuous formation and destruction of a thin surface oxide (possibly creating mesoscopic roughness due to the etching of metal particles from the oxide framework^{13,42}), how would one be able to distinguish what is an oxide vacancy, what the oxide, what an oxygen atom diffusing on or below the metal surface, let alone determine whether this would show up in a unique kinetics that would still be describable by simple macroscopic rate equations?

In this regard, another intriguing result of our thermodynamic considerations is the different stability range of surface oxides on Pd(111) and Pd(100). Again, provided the catalyst is close to thermodynamic equilibrium, this would imply that under certain (T, p) -conditions the active phase for CO oxidation could be on-surface adphases (i.e. LH) on some facets of nanoparticles and surface oxides (let's call this MvK) on others. A situation that could make the overall kinetic data (and its modelling) much more complex than hitherto assumed. In this particular sense, an understanding of the data from Pd could be much more difficult than say for Ag, where we would not expect neither bulk nor surface oxides to play a significant role in CO oxidation catalysis on the basis of the present results, and in agreement with the conclusions of a more detailed recent theoretical study¹⁵.

VI. SUMMARY

In conclusion we have derived simple thermodynamic stability conditions for bulk and surface oxides in contact with an environment formed of CO and O₂. Applying these to the late 4*d* transition metal series from Ru to Ag, we obtain a progressively smaller stability range for the bulk oxides that extends well into the environmental conditions representative of technological CO oxidation catalysis only in the case of RuO₂. In particular for Pd, thin surface oxides could nevertheless still be stable in the more oxygen-rich part of this (T, p) -range, while for CO containing gas phases neither surface nor bulk oxide will be stable on Ag. Most intriguingly, oscillations between metal and bulk (surface) oxide phase for Rh (Pd) are conceivable under technologically relevant (T, p) -conditions.

Provided the catalyst is close to the constrained thermodynamic equilibrium forming the basis of our considerations, these results may give first insight into the role of oxide formation played in technological CO oxidation catalysis at these 4*d* TMs. A comprehensive understanding of the microscopic state and full catalytic cycle must however be based on statistical mechanics as the next step, i.e. by modelling the very dynamic behavior and interplay of the manifold of elementary processes.

Acknowledgments

We acknowledge detailed discussions with Cathy Stampfl and Weixue Li on the Ag/Ag₂O system and with

Mira Todorova on the Pd/PdO system. K.R. is grateful for financial support from the Deutsche Forschungsgemeinschaft (DFG). We thank Mark Miller for a careful reading of the manuscript.

-
- ¹ K.C. Taylor, Catal. Rev.-Sci. Eng. **35**, 457 (1993).
² S.H. Oh and J.E. Carpenter, J. Catal. **80**, 472 (1983).
³ G.L. Kellogg, Phys. Rev. Lett. **54**, 82 (1985); Surf. Sci. **171**, 359 (1986).
⁴ C.H.F. Peden, D.W. Goodman, D.S. Blair, P.J. Berlowitz, G.B. Fisher, and S.H. Oh, J. Phys. Chem. **92**, 1563 (1988).
⁵ J.E. Turner, B.C. Sales, and M.B. Maple, Surf. Sci. **103**, 54 (1981); *ibid.* **109**, 591 (1981).
⁶ V.A. Bondzie, P. Kleban, and D. J. Dwyer, Surf. Sci. **347**, 319 (1996).
⁷ M. Ziauddin, G. Vesper, and L. D. Schmidt, Catal. Lett. **46**, 159 (1997).
⁸ G. Vesper, A. Wright, and R. Caretta, Catal. Lett. **58**, 199 (1999).
⁹ C. Stampfl, M.V. Ganduglia-Pirovano, K. Reuter, and M. Scheffler, Surf. Sci. **500**, 368 (2002).
¹⁰ H. Over, Y.D. Kim, A.P. Seitsonen, S. Wendt, E. Lundgren, M. Schmid, P. Varga, A. Morgante, and G. Ertl, Science **287**, 1474 (2000).
¹¹ Y.D. Kim, H. Over, G. Krabbes, and G. Ertl, Topics in Catalysis **14**, 95 (2001).
¹² B.L.M. Hendriksen, S.C. Bobaru, and J.W.M. Frenken, Surf. Sci. (*submitted*).
¹³ B.L.M. Hendriksen, *Model Catalysts in Action: High-Pressure Scanning Tunneling Microscopy*, Ph.D. thesis, Universiteit Leiden (2003).
¹⁴ C.I. Carlisle, D.A. King, M.L. Boucquet, J. Cerdá, and P. Sautet, Phys. Rev. Lett. **84**, 3899 (2000).
¹⁵ W.X. Li, C. Stampfl, and M. Scheffler, Phys. Rev. B **67**, 045408 (2003); and to be published.
¹⁶ C.M. Weinert and M. Scheffler, In: *Defects in Semiconductors*, H.J. von Bardeleben (Ed.), Mat. Sci. Forum **10-12**, 25 (1986). <http://www.fhi-berlin.mpg.de/th/publications/Mat-Sci-Forum-10-12-1986.pdf>.
¹⁷ M. Scheffler, In: *Physics of Solid Surfaces - 1987*, J. Koukal (Ed.), Elsevier, Amsterdam (1988). <http://www.fhi-berlin.mpg.de/th/publications/Phys-of-Sol-Surfaces-1987-1988.pdf>.
¹⁸ M. Scheffler and J. Dabrowski, Phil. Mag. A **58**, 107 (1988). <http://www.fhi-berlin.mpg.de/th/publications/Phil-Mag-A-58-107-1988.pdf>.
¹⁹ E. Kaxiras, Y. Bar-Yam, J.D. Joannopoulos, and K.C. Pandey, Phys. Rev. B **35**, 9625 (1987).
²⁰ G.-X. Qian, R.M. Martin, and D.J. Chadi, Phys. Rev. B **38**, 7649 (1988).
²¹ X.-G. Wang, W. Weiss, Sh.K. Shaikhutdinov, M. Ritter, M. Petersen, F. Wagner, R. Schlögl, and M. Scheffler, Phys. Rev. Lett. **81**, 1038 (1998).
²² X.-G. Wang, A. Chaka, and M. Scheffler, Phys. Rev. Lett. **84**, 3650 (2000).
²³ K. Reuter and M. Scheffler, Phys. Rev. B **65**, 035406 (2002).
²⁴ K. Reuter and M. Scheffler, Phys. Rev. Lett. **90**, 046103 (2003).
²⁵ K. Reuter and M. Scheffler, Phys. Rev. B (*submitted*); cond-mat/0301602.
²⁶ D.R. Stull and H. Prophet, *JANAF Thermochemical Tables*, 2nd ed., U.S. National Bureau of Standards, Washington, D.C. (1971).
²⁷ K. Reuter and M. Scheffler, (to be published).
²⁸ CRC Handbook of Chemistry and Physics, 76th ed. (CRC Press, Boca Raton, FL 1995).
²⁹ M.E. Grillo, M.V. Ganduglia-Pirovano, and M. Scheffler, (*unpublished results*).
³⁰ J. Rogal, M. Todorova, K. Reuter, and M. Scheffler (*to be published*).
³¹ E. Lundgren, G. Kresse, C. Klein, M. Borg, J.N. Andersen, M. De Santis, Y. Gauthier, C. Konvicka, M. Schmid, and P. Varga, Phys. Rev. Lett. **88**, 246103 (2002).
³² M. Todorova, E. Lundgren, V. Blum, A. Mikkelsen, S. Gray, J. Gustafson, M. Borg, J. Rogal, K. Reuter, J.N. Andersen, and M. Scheffler, Surf. Sci. (*in preparation*).
³³ M. Todorova, K. Reuter, and M. Scheffler (*to be published*).
³⁴ D. Kolthoff, D. Jürgens, C. Schwennicke, and H. Pfnür, Surf. Sci. **365**, 374 (1996).
³⁵ G. Zheng and E.I. Altman, Surf. Sci. **504**, 253 (2002).
³⁶ J. Szanyi, W.K. Kuhn, and D.W. Goodman, J. Vac. Sci. Techn. A **11**(4), 1969 (1993).
³⁷ K. Reuter, C. Stampfl, M.V. Ganduglia-Pirovano, and M. Scheffler, Phys. Rev. Lett. **352**, 311 (2002).
³⁸ K. Reuter, M.V. Ganduglia-Pirovano, C. Stampfl, and M. Scheffler, Phys. Rev. B **65**, 165403 (2002).
³⁹ B.L.M. Hendriksen, M.D. Ackermann, and J.W.M. Frenken, Surf. Sci. (*submitted*).
⁴⁰ R.I. Masel, *Principles of Adsorption and Reaction on Solid Surfaces*, Wiley, New York (1996).
⁴¹ P. I. Barteaux and D.W. van Krevelen, Chem. Eng. Sci. **3**, 41 (1954).
⁴² G. Ertl, H. Knözinger, and J. Weitkamp (Eds.), *Handbook of Heterogeneous Catalysis*, Wiley, New York (1997).
⁴³ B.L.M. Hendriksen und J.W.M. Frenken, Phys. Rev. Lett. **89**, 046101 (2002).